Table 3
Echocardiographic measurements in TAC-APA5 or TAC-IgG mice

	TAC-IgG	TAC-APA5
Number	10	10
HW/BW (mg/g)	5.71 ± 0.18	5.67 ± 0.16
HR (bpm)	633.30 ± 16.06	657.00 ± 11.91
LVDd (mm)	3.54 ± 0.09	3.59 ± 0.08
LVDs (mm)	2.07 ± 0.09	2.01 ± 0.09
FS (%)	41.7 ± 1.48	44.2 ± 1.51
LVPWth (mm)	0.84 ± 0.01	0.81 ± 0.01

Mast cell stabilization and BM reconstitution. For stabilization of mast cells, cromolyn (50 mg/kg/day; Sigma-Aldrich) or vehicle was administrated daily to mice by i.p. injection (14) for the duration of the experiment (10 days after TAC operation). For BM reconstitution, BM cell suspensions were harvested by flushing the femurs and tibias of 8-week-old W/W^v or +/+ mice. The 5-week-old C57BL/6 mice were preconditioned with total body irradiation (9.5 Gy) 6 hours before transplantation. BM cell suspensions (1.0 × 10^7 cells per mouse) were transfused via the tail vein to the preconditioned recipient mice. The recipient mice were subjected to BM reconstitution for 6 weeks and were subjected to TAC operation.

Induction of AF in ex vivo and in vivo hearts. For induction of AF in ex vivo hearts, hearts were rapidly excised after i.p. injection of heparin (0.5 U/g) and urethane (2 mg/g) and immediately mounted onto a Langendorff perfusion apparatus (42). The hearts were perfused with a nonrecirculating Krebs-Henseleit buffer (119 mM NaCl, 4.8 mM KCl, 1.2 mM KH$_2$PO$_4$, 1.2 mM MgSO$_4$, 2.5 mM CaCl$_2$, 10 mM glucose, and 24.9 mM NaHCO$_3$), which was equilibrated with 5% CO$_2$/95% O$_2$ at 37°C. All isolated hearts were stabilized for 5 minutes by perfusion at constant flow (3.0 ± 0.2 ml/min) before programmed electrical stimulation. The whole system temperature was kept at 37°C. Two chlorinated silver wires were placed on the base of the heart as indifferent and common ground electrodes. A pair of recording electrodes were placed on the apex and anterior wall of the heart to record ventricular electrograms. Bipolar stimulating electrodes were pressed against the right atrium surface, and bipolar recording electrodes were placed on the left atrium surface to record atrial electrograms.

For induction of AF in in vivo hearts, mice were anesthetized with i.p. injection of pentobarbital and supported by artificial ventilation. The body temperature of mice was monitored and kept at 37°C using a heating pad during the experiments. A 2-French catheter electrode (Japan Lifeline) was placed at the esophageal position dorsal to the left atrium. A surface ECG was simultaneously recorded using electrodes in a lead-II configuration.

Inducibility of AF was tested by applying a 2-second burst using the automated stimulator. The first 2-second burst had a cycle length (CL) of 40 ms, decreasing in each successive burst with a 2-microsecond decrement down to a CL of 20 ms. A series of bursts was repeated 3 times after stabilization for 5 minutes. AF duration was defined as the interval between the rapid irregular atrial rhythm triggered after the bursts and the onset of first normal sinus beat.

Histological analysis. Hearts were excised and immediately fixed in 10% neutralized formalin, and they were then embedded in paraffin. Serial sections of atrium at 5 μm were stained with Masson's trichrome for evaluation of fibrosis. We determined mast cell number and morphology with toluidine blue staining (0.1%; Sigma-Aldrich) and rhodamine-avidin staining (1:100; Vector Laboratories) (20, 26). Specificity of mast cell detection was confirmed by staining sections of W/W^v and +/+ mice at the same dilution of the reagent. The total number of mast

cells was counted manually and blindly in 3 microscopic sections from each mouse, and the total area was determined using computer-assisted image analysis (ImageJ; http://rsbweb.nih.gov/ij/).

Hydroxyproline assay. We evaluated collagen content in the atrium by quantification of hydroxyproline, as described previously (43). In brief, the atrium was weighed and then hydrolyzed in 6 N HCl at 100°C overnight. Hydrolyzed tissue was neutralized with NaOH, vacuum dried at 50°C, and resuspended in 1 ml of 5 mM HCl. An aliquot of 20 μl hydrolyzed tissue was added to 180 μl of H$_2$O in a glass tube. Thereafter, we mixed 100 μl of chloramine-T solution (0.14 g chloramine-T, Sigma-Aldrich; 2 ml H$_2$O, 8 ml hydroxyproline assay buffer) with the diluted hydrolyzed tissue solution. The ingredients of hydroxyproline assay buffer were as follows: 11.4 g sodium acetate anhydrous (Sigma-Aldrich), 7.5 g trisodium citrate dihydrate (Sigma-Aldrich), 40 ml H$_2$O (pH adjusted to 6.0), and 77 ml isopropanol, bringing the final volume to 200 ml with H$_2$O. After incubation for 10 minutes at room temperature, 1.25 ml Ehrlich's reagent (6.0 g p-dimethylaminobenzaldehyde [Sigma-Aldrich], 18 ml 60% perchlorate [Fluka], 78 ml isopropanol) was added and mixed. The samples were incubated at 55°C for 20–25 minutes, and the sample absorbance was read at 558 nm. We used trans-4-hydroxy-L-proline (Sigma-Aldrich) (ranging from 0 to 4 mg) to draw the standard curve.

Coculture of BMMCs with cardiac myocytes or fibroblasts. The BM cells were harvested from C57BL/6 mice and cultured for 5 weeks in RPMI 1640 medium (GIBCO; Invitrogen) supplemented with 10% FBS (Equitech-Bio), 0.1 mM MEM Non-Essential Amino Acids Solution (GIBCO; Invitrogen), 4 mM L-glutamine, 25 mM HEPES, 1 mM sodium pyruvate, 50 μM β-mercaptoethanol, 100 U/ml penicillin, 100 μg/ml streptomycin, and 30 ng/ml of recombinant murine IL-3 (PeproTech GmbH) at 37°C in 5% CO$_2$ (44). By 5 weeks in culture, mast cells were enriched to more than 95%, as assessed by the presence of metachromatic granules in toluidine blue–stained cells and by cell-surface expression of FcεRI (Upstate) using flow cytometric analysis. The cardiac myocytes and fibroblasts were prepared from hearts of 1-day-old Wistar rats, as described previously (45). Dissociated cells were preplated onto 10-cm culture dishes for 30 minutes, which permitted preferential attachment of fibroblasts to the bottom of the dish. Nonadherent cardiac myocytes (3.5 × 10^5 cells/3.5-cm dish) or adherent fibroblasts (2.0 × 10^6 cells/3.5-cm dish) were plated on 3.5-cm dishes and cultured for 24 hours in medium (DMEM [GIBCO; Invitrogen], supplemented with 10% FBS, 100 U/ml penicillin, and 100 μg/ml streptomycin). The cells were starved under a serum-free condition for 24 hours before initiation of the coculture. BMMCs (5.0 × 10^6 cells/3.5-cm dish) were placed onto layers of cardiac myocytes or fibroblasts and were continuously cocultured in DMEM without supplementation with FBS. For stabilization of BMMCs in vitro, BMMCs were pretreated with 10^{-5} M cromolyn (Sigma-Aldrich) for 30 minutes before initiation of coculture, and cromolyn treatment was continued throughout the coculture.

Real-time RT-PCR analysis. Total RNA was extracted by using RNeasy Kit (QIAGEN), and single-stranded cDNA was transcribed by using QuantiTect Reverse Transcription Kit (QIAGEN) according to the manufacturer's protocol. We conducted quantitative real-time PCR analysis with the Universal ProbeLibrary Assays (Roche Applied Science) according to the manufacturer's instructions. Amplification conditions were as follows: initial denaturation for 10 minutes at 95°C followed by 45 cycles of 10 seconds at 95°C and 25 seconds at 60°C. Individual PCR products were analyzed by melting-point analysis. The expression level of a gene was normalized relative to that of *Gapdh* by using a comparative Ct method. The primer sequences and universal probe numbers were designed with the ProbeFinder software as follows: *Pdgfa*, 5'-GTGCGACCTCCAACCTGA-3' and 5'-GGCTCATCT-CACCTCACATCT-3', no. 52; *Pdgfb*, 5'-CGGCCTGTGACTAGAAGTCC-3' and 5'-GAGCTTGAGGCGTCTTGG-3', no. 32; *Col3a1*, 5'-TCCCCTG-
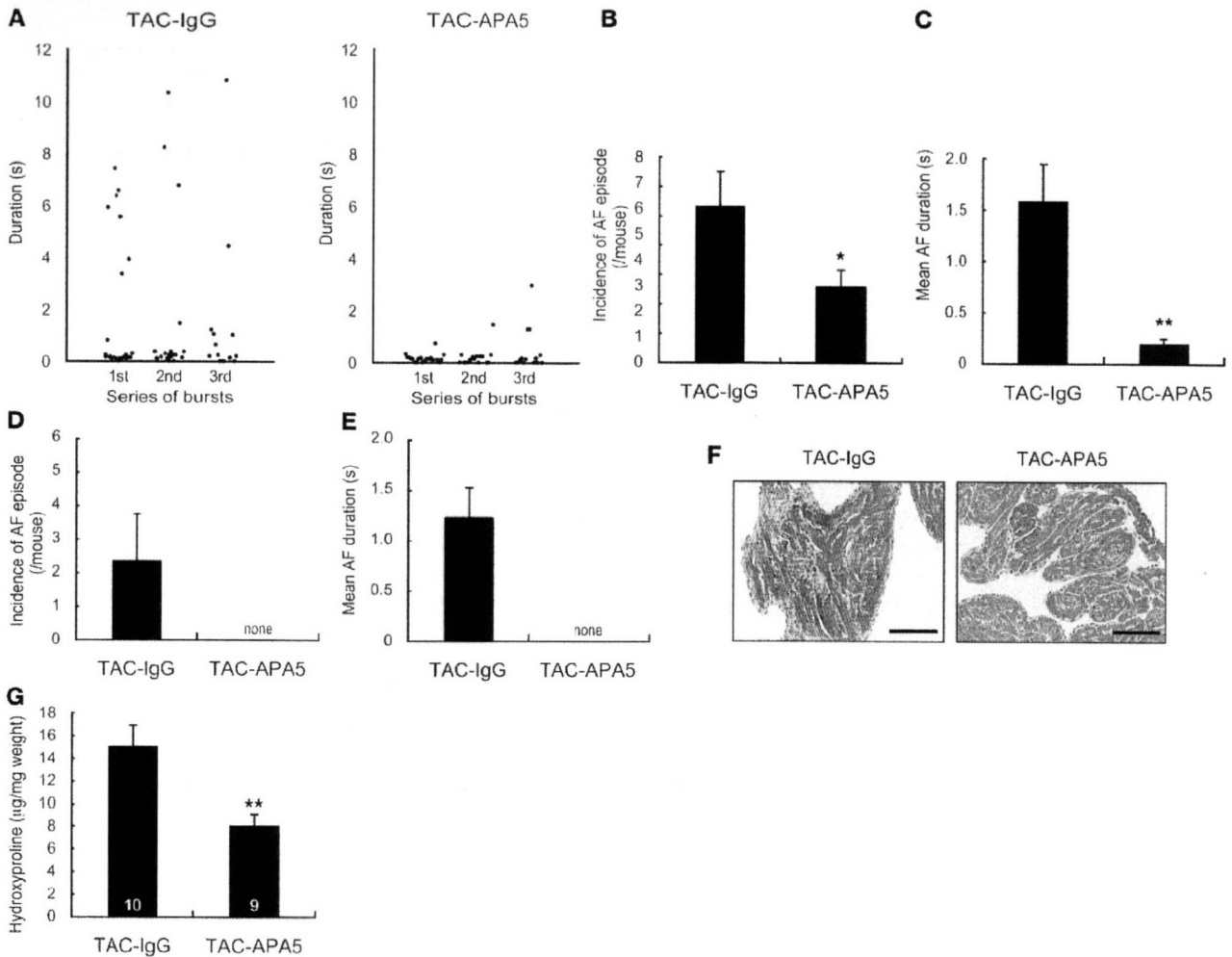
Figure 8
Attenuation of atrial fibrosis and AF by neutralization of PDGFR-α. (**A**) Scatter plot of duration of AF episodes occurring during 3 series of bursts under Langendorff perfusion in TAC-APA5 ($n = 9$) or TAC-IgG mice ($n = 9$). (**B**) Incidence of AF episodes during 3 series of bursts under Langendorff perfusion ($n = 9$). *$P < 0.05$ versus control IgG. (**C**) Mean duration of AF episodes during 3 series of bursts under Langendorff perfusion ($n = 9$). **$P < 0.01$ versus control IgG. (**D**) Incidence of AF episodes during 3 series of transesophageal bursts ($n = 6$). (**E**) Mean duration of AF episodes during 3 series of transesophageal bursts ($n = 6$). (**F**) Representative histological sections with Masson's trichrome staining for visualization of atrial fibrosis (blue staining). Scale bars: 20 μm. (**G**) Hydroxyproline content in the atrium ($n = 9$). Number of mice for each experiment is indicated in the bars. **$P < 0.01$ versus control IgG. Data are presented as mean ± SEM.

GAATCTGTGAATC-3′ and 5′-TGAGTCGAATTGGGGAGAAT-3′, no. 49; mouse *Gapdh*, 5′-TGTCCGTCGTGGATCTGAC-3′ and 5′-CCTGCTTCAC-CACCTTCTTG-3′, no. 80; rat *Gapdh*, 5′-TGGGAAGCTGGTCATCAAC-3′ and 5′-GCATCACCCCATTTGATGTT-3′, no. 9.

ELISA of PDGF-AA. The concentrations of PDGF-AA in the conditioned medium were assayed by using Human/Mouse PDGF-AA Quantikine ELISA Kit (R&D Systems) according to the manufacturer's protocol.

Cell proliferation assay. Cardiac fibroblasts (2×10^4 cells/well) were plated on a 48-well plate and were cultured for 24 hours in medium (DMEM supplemented with 10% FBS, 100 U/ml penicillin, and 100 μg/ml streptomycin) at 37°C in 5% CO_2. After 24 hours of starvation under serum-free conditions, we replaced the medium with that conditioned by coculture of BMMCs and cardiac fibroblasts. After 24 hours of culture, cells were harvested, and subjected to semiquantification of the viable cell numbers that are proportional to the amount of ATP by using CellTiter-Glo Luminescent Cell Viability Assay Kit (Promega).

Systemic administration of PDGF-AA. Mini-osmotic pumps (model 2002; Alzet) were subcutaneously implanted in 10-week-old male mice to deliver recombinant murine PDGF-AA (0.2 μg/day; PeproTech) or vehicle. At 10 days after implantation, mice were sacrificed for analysis.

Inhibition of PDGF-A by a neutralizing anti–PDGFR-α antibody. To antagonize the effects of BMMC-derived PDGF-A in vitro, we pretreated BMMCs with 2 μg/ml of clone APA5 (200 μg/day) (27) or control IgG2a (eBioscience) for 30 minutes before initiation of coculture and continued the treatment throughout the coculture. To inhibit the effects of PDGF-A in vivo, we administered anti–PDGFR-α antibody (200 μg/day) (27) or control IgG2a by i.p. injection to mice for the duration of the experiment (10 days after TAC operation). APA5, a rat monoclonal anti-mouse PDGFR-α antibody (IgG2a), was described previously (46).

Statistics. All data are presented as means ± SEM. Two-group comparison was analyzed by unpaired 2-tailed Student's *t* test, and multiple-group comparison was performed by 1-way ANOVA followed by the Fisher's pro-

tected least significant difference test for comparison of means. $P < 0.05$ was considered to be statistically significant.

Address correspondence to: Issei Komuro, Department of Cardiovascular Science and Medicine, Chiba University Graduate School of Medicine, 1-8-1 Inohana, Chuo-ku, Chiba 260-8670, Japan. Phone: 81-43-226-2097; Fax: 81-43-226-2557; E-mail: komuro-tky@umin.ac.jp.

1. Fuster V, et al. ACC/AHA/ESC 2006 guidelines for the management of patients with atrial fibrillation. *Circulation.* 2006;114(7):e257-354.
2. Nattel S. New ideas about atrial fibrillation 50 years on. *Nature.* 2002;415(6868):219-226.
3. Burstein B, Nattel S. Atrial fibrosis: mechanisms and clinical relevance in atrial fibrillation. *J Am Coll Cardiol.* 2008;51(8):802-809.
4. Corradi D, Callegari S, Maestri R, Benussi S, Alfieri O. Structural remodeling in atrial fibrillation. *Nat Clin Pract Cardiovasc Med.* 2008;5(12):782-796.
5. Frustaci A, et al. Histological substrate of atrial biopsies in patients with lone atrial fibrillation. *Circulation.* 1997;96(4):1180-1184.
6. Issac TT, Dokainish H, Lakkis NM. Role of inflammation in initiation and perpetuation of atrial fibrillation: a systematic review of the published data. *J Am Coll Cardiol.* 2007;50(21):2021-2028.
7. Nakamura Y, et al. Tissue factor expression in atrial endothelia associated with nonvalvular atrial fibrillation: possible involvement in intracardiac thrombogenesis. *Thromb Res.* 2003;111(3):137-142.
8. Verheule S, et al. Alterations in atrial electrophysiology and tissue structure in a canine model of chronic atrial dilatation due to mitral regurgitation. *Circulation.* 2003;107(20):2615-2622.
9. Chung MK, et al. C-reactive protein elevation in patients with atrial arrhythmias: inflammatory mechanisms and persistence of atrial fibrillation. *Circulation.* 2001;104(24):2886-2891.
10. Aviles RJ, et al. Inflammation as a risk factor for atrial fibrillation. *Circulation.* 2003;108(24):3006-3010.
11. Kalesnikoff J, Galli SJ. New developments in mast cell biology. *Nat Immunol.* 2008;9(11):1215-1223.
12. Metz M, Grimbaldeston MA, Nakae S, Piliponsky AM, Tsai M, Galli SJ. Mast cells in the promotion and limitation of chronic inflammation. *Immunol Rev.* 2007;217:304-328.
13. Sperr WR, et al. The human cardiac mast cell: localization, isolation, phenotype, and functional characterization. *Blood.* 1994;84(11):3876-3884.
14. Bot I, et al. Perivascular mast cells promote atherogenesis and induce plaque destabilization in apolipoprotein E-deficient mice. *Circulation.* 2007;115(19):2516-2525.
15. Sun J, et al. Mast cells promote atherosclerosis by releasing proinflammatory cytokines. *Nat Med.* 2007;13(6):719-724.
16. Sun J, et al. Mast cells modulate the pathogenesis of elastase-induced abdominal aortic aneurysms in mice. *J Clin Invest.* 2007;117(11):3359-3368.
17. Tsuruda T, et al. Adventitial mast cells contribute to

pathogenesis in the progression of abdominal aortic aneurysm. *Circ Res.* 2008;102(11):1368-1377.
18. Hara M, et al. Evidence for a role of mast cells in the evolution to congestive heart failure. *J Exp Med.* 2002;195(3):375-381.
19. Higuchi H, et al. Mast cells play a critical role in the pathogenesis of viral myocarditis. *Circulation.* 2008;118(4):363-372.
20. Mackins CJ, et al. Cardiac mast cell-derived renin promotes local angiotensin formation, norepinephrine release, and arrhythmias in ischemia/reperfusion. *J Clin Invest.* 2006;116(4):1063-1070.
21. Cairns JA, Walls AF. Mast cell tryptase stimulates the synthesis of type I collagen in human lung fibroblasts. *J Clin Invest.* 1997;99(6):1313-1321.
22. Kondo S, et al. Role of mast cell tryptase in renal interstitial fibrosis. *J Am Soc Nephrol.* 2001;12(8):1668-1676.
23. Mori R, Shaw TJ, Martin P. Molecular mechanisms linking wound inflammation and fibrosis: knockdown of osteopontin leads to rapid repair and reduced scarring. *J Exp Med.* 2008;205(1):43-51.
24. Theoharides TC, Kempuraj D, Tagen M, Conti P, Kalogeromitros D. Differential release of mast cell mediators and the pathogenesis of inflammation. *Immunol Rev.* 2007;217:65-78.
25. Sano M, et al. p53-induced inhibition of Hif-1 causes cardiac dysfunction during pressure overload. *Nature.* 2007;446(7134):444-448.
26. Tharp MD, Seelig LL Jr, Tigelaar RE, Bergstresser PR. Conjugated avidin binds to mast cell granules. *J Histochem Cytochem.* 1985;33(1):27-32.
27. Zymek P, et al. The role of platelet-derived growth factor signaling in healing myocardial infarcts. *J Am Coll Cardiol.* 2006;48(11):2315-2323.
28. Olgin JE, Verheule S. Transgenic and knockout mouse models of atrial arrhythmias. *Cardiovasc Res.* 2002;54(2):280-286.
29. Kitamura Y, Go S, Hatanaka K. Decrease of mast cells in W/Wv mice and their increase by bone marrow transplantation. *Blood.* 1978;52(2):447-452.
30. Huizinga JD, et al. W/kit gene required for interstitial cells of Cajal and for intestinal pacemaker activity. *Nature.* 1995;373(6512):347-349.
31. Li M, et al. c-kit is required for cardiomyocyte terminal differentiation. *Circ Res.* 2008;102(6):677-685.
32. Lewis JP, O'Grady LF, Bernstein SE, Russell EE, Trobaugh FE, Jr. Growth and differentiation of transplanted W/Wv marrow. *Blood.* 1967;30(5):601-616.
33. Patella V, et al. Stem cell factor in mast cells and increased mast cell density in idiopathic and ischemic cardiomyopathy. *Circulation.*

1998;97(10):971-978.
34. Galli SJ, et al. Mast cells as "tunable" effector and immunoregulatory cells: recent advances. *Annu Rev Immunol.* 2005;23:749-786.
35. Thompson HL, Burbelo PD, Segui-Real B, Yamada Y, Metcalfe DD. Laminin promotes mast cell attachment. *J Immunol.* 1989;143(7):2323-2327.
36. Dastych J, Costa JJ, Thompson HL, Metcalfe DD. Mast cell adhesion to fibronectin. *Immunology.* 1991;73(4):478-484.
37. Bianchine PJ, Burd PR, Metcalfe DD. IL-3-dependent mast cells attach to plate-bound vitronectin. Demonstration of augmented proliferation in response to signals transduced via cell surface vitronectin receptors. *J Immunol.* 1992;149(11):3665-3671.
38. Bonner JC. Regulation of PDGF and its receptors in fibrotic diseases. *Cytokine Growth Factor Rev.* 2004;15(4):255-273.
39. Burstein B, Libby E, Calderone A, Nattel S. Differential behaviors of atrial versus ventricular fibroblasts: a potential role for platelet-derived growth factor in atrial-ventricular remodeling differences. *Circulation.* 2008;117(13):1630-1641.
40. Kumagai K, et al. Effects of angiotensin II type 1 receptor antagonist on electrical and structural remodeling in atrial fibrillation. *J Am Coll Cardiol.* 2003;41(12):2197-2204.
41. Nattel S, Shiroshita-Takeshita A, Brundel BJ, Rivard L. Mechanisms of atrial fibrillation: lessons from animal models. *Prog Cardiovasc Dis.* 2005;48(1):9-28.
42. Suzuki M, et al. Functional roles of cardiac and vascular ATP-sensitive potassium channels clarified by Kir6.2-knockout mice. *Circ Res.* 2001;88(6):570-577.
43. Oka T, et al. Cardiac-specific deletion of Gata4 reveals its requirement for hypertrophy, compensation, and myocyte viability. *Circ Res.* 2006;98(6):837-845.
44. Jensen BM, Swindle EJ, Iwai S, Gilfillan AM. Generation, isolation, and maintenance of rodent mast cells and mast cell lines. In Coligan, JE, Bierer, B, Margulies, DH, Shevach, EM, Strober, W, Coico, R, eds. *Current Protocols in Immunology.* Hoboken, NJ: John Wiley & Sons; 2006:Chapter 3:Unit 3.23.
45. Zou Y, et al. Cell type-specific angiotensin II-evoked signal transduction pathways: critical roles of Gbetagamma subunit, Src family, and Ras in cardiac fibroblasts. *Circ Res.* 1998;82(3):337-345.
46. Takakura N, Yoshida H, Kunisada T, Nishikawa S, Nishikawa SI. Involvement of platelet-derived growth factor receptor-alpha in hair canal formation. *J Invest Dermatol.* 1996;107(5):770-777.

Inhibition of Semaphorin As a Novel Strategy for Therapeutic Angiogenesis

Junji Moriya,* Tohru Minamino,* Kaoru Tateno, Sho Okada, Akiyoshi Uemura, Ippei Shimizu, Masataka Yokoyama, Aika Nojima, Mitsuhiro Okada, Hisashi Koga, Issei Komuro

Rationale: The axon-guiding molecules known as semaphorins and their receptors (plexins) regulate the vascular pattern and play an important role in the development of vascular network during embryogenesis. Semaphorin (Sema)3E is one of the class 3 semaphorins, and plexinD1 is known to be its receptor. Although these molecules have a role in embryonic vascular development, it remains unclear whether the Sema3E/plexinD1 axis is involved in postnatal angiogenesis.

Objective: The objective of this study was to elucidate the role of Sema3E/plexinD1 in postnatal angiogenesis.

Methods and Results: Sema3E inhibited cell growth and tube formation by suppressing the vascular endothelial growth factor (VEGF) signaling pathway. Expression of Sema3E and plexinD1 was markedly upregulated in ischemic limbs of mice (2.5- and 4.5-fold increase for Sema3E and plexinD1, respectively), and inhibition of this pathway by introduction of the plexinD1-Fc gene or disruption of Sema3E led to a significant increase of blood flow recovery (1.6- and 1.5-fold increase for the plexinD1-Fc gene treatment and Sema3E disruption, respectively). Hypoxia activated the tumor suppressor protein p53, thereby upregulating Sema3E expression. Expression of p53 and Sema3E was enhanced in diabetic mice compared with normal mice (2- and 1.3-fold increase for p53 and Sema3E, respectively). Consequently, neovascularization after VEGF treatment was poor in the ischemic tissues of diabetic mice, whereas treatment with VEGF plus plexinD1-Fc markedly improved neovascularization.

Conclusions: These results indicate that inhibition of Sema3E may be a novel strategy for therapeutic angiogenesis, especially when VEGF is ineffective. (*Circ Res.* 2010;106:391-398.)

Key Words: angiogenesis ■ semaphorins ■ p53 ■ diabetes

The vascular system and nervous system have several striking anatomic similarities. Recent findings have shown that the similarities between these systems extend to the molecular level and that the molecular mechanisms which are important for the specification, differentiation, and patterning of nerves also play an important role within the vasculature and vice versa.[1-4] Development of the nervous system is regulated through the coordinated action of a variety of repulsive or attractive neuronal guidance factors, called "axon-guiding molecules," that direct the growth of axons into specific pathways.[3] Recently, these axon-guiding molecules (including semaphorins) have also been shown to play a pivotal role in the formation of vascular networks.[1,5]

Semaphorins and their receptors (known as plexins) were initially characterized as signaling molecules that repel or attract axons,[6-9] but are now recognized as critical regulators of morphogenesis and homeostasis in various organs and systems.[10,11] The semaphorin family comprises 21 genes in vertebrates and eight additional genes are found in invertebrates. These genes are divided into eight classes on the basis of the similarity of their structural domains, with classes 3 to 7 containing the vertebrate semaphorins.[5] Class 3 are the only semaphorins secreted in vertebrates. Semaphorin (Sema)3E is one of the class 3 semaphorins,[12] and plexinD1 is known to be its receptor.[10] It has been reported that loss of plexinD1 or Sema3E causes abnormalities of vascular growth,[10] suggesting that these molecules have a crucial role in regulating the pattern of vessel development during embryogenesis.[13,14] However, it remains unknown whether Sema3E and plexinD1 are involved in postnatal angiogenesis.

DOI: 10.1161/CIRCRESAHA.109.210815

Non-standard Abbreviations and Acronyms	
ERK	extracellular signal-regulated kinase
HUVEC	human umbilical vein endothelial cell
Sema	semaphorin
VEGF	vascular endothelial growth factor
VEGFR	vascular endothelial growth factor receptor

In this study, we performed both in vivo and in vitro investigations into the role of Sema3E/plexinD1 in postnatal angiogenesis, and we found that these 2 molecules inhibit angiogenesis by suppressing the vascular endothelial growth factor (VEGF) signaling pathway. Sema3E expression was upregulated in ischemic tissue via a p53-dependent pathway. Its upregulation was further enhanced in a diabetic model, attenuating the effect of VEGF treatment, whereas inhibition of Sema3E markedly improved the response to VEGF. These findings suggest that inhibition of Sema3E may be a novel strategy for therapeutic angiogenesis, especially when VEGF is ineffective.

Methods

Cell Culture

Recombinant human VEGF165 (293-VE), monoclonal antihuman VEGF antibody (MAB293) and recombinant human Sema3E were purchased from R&D Systems (Minneapolis, Minn). PlexinD1 Fc protein was generated by ARK Resource (Kumamoto, Japan). Human umbilical vein endothelial cells (HUVECs) were purchased from BioWhittaker (Walkersville, Md) and cultured according to the instructions of the manufacturer. Endothelial cell proliferation was assessed by determining cell counts after culture in the presence of VEGF165 (50 ng/mL) for 2 days. Retroviral stocks were generated by transient transfection of packaging cell line (PT67, Clontech) and stored at $-80°C$ until use. Human endothelial cells (passage 4 to 6) were plated at $5×10^5$ cells per 100-mm-diameter dish 24 hours before infections. For infections, the culture medium was replaced by retroviral stocks supplemented with 8 μg/mL polybrene (Sigma, Tokyo, Japan). Forty-eight hours after infections, the infected cell populations were selected by culture in 0.8 μg/mL puromycin for 4 days. High-titer adenoviral stocks (10^9 pfu) were generated with the Adeno-X Expression System (Clontech) according to the instructions of the manufacturer.

Tube-Formation Assay

The tube-formation assay was performed using a commercially available kit according to the manufacturer's instructions (Kurabo, Osaka, Japan). HUVECs were cultured for 11 days in the presence of VEGF165 (10 ng/mL) and test substances, after which they were fixed at room temperature in 70% ethanol. The fixed cells were then incubated first with mouse antihuman CD31 antibody (1:4000 dilution) for 1 hour and then with a goat anti-mouse IgG alkaline phosphatase–conjugated secondary antibody, which was visualization using 5-bromo-4-chloro-3-indolyl phosphate/nitro blue tetrazolium. Capillary-like tube formation was assessed by photography under an inverted phase contrast microscope at a ×40 magnification. The vessel area was defined as the area of CD31-positive cells / total area, which was estimated by an angiogenesis image analyzer (Kurabo, Osaka, Japan). This assay was performed in triplicate.

Western Blot Analysis

Whole cell lysates were prepared in lysis buffer (10 mmol/L Tris-HCl, pH 8, 140 mmol/L NaCl, 5 mmol/L EDTA, 0.025% NaN3, 1% Triton X-100, 1% deoxycholate, 0.1% SDS, 1 mmol/L PMSF, 5 μg/mL leupeptin, 2 μg/mL aprotinin, 50 mmol/L NaF, and 1 mmol/L Na_2VO_3). The lysates (30 to 50 μg) were resolved by SDS-PAGE. Proteins were transferred to a poly(vinylidene difluoride) membrane (Millipore, Bedford, Mass) and incubated with the primary antibody followed by anti-rabbit IgG–horseradish peroxidase antibody or anti-mouse IgG–horseradish peroxidase antibody or anti-goat IgG–horseradish peroxidase antibody (Jackson, West Grove, Pa). Specific proteins were detected by using enhanced chemiluminescence (Amersham, Buckinghamshire, UK). Immunoprecipitation was performed as described previously.[15] The primary antibodies used for Western blotting were as follows; anti–phospho–extracellular signal-regulated kinase (ERK) antibody (sc-7383), anti-ERK antibody (sc-154-G), anti-pAkt antibody (sc-7985-R), anti-Akt antibody (sc-1618), anti-p53 antibody (sc-126, sc-99), anti-actin antibody (sc-8432), anti–flk-1 antibody (sc-6251), anti-Sema3E antibody (sc-49733) (Santa Cruz Biotechnology, Santa Cruz, Calif), and anti-phosphotyrosine antibody (4G10) (Upstate, Lake Placid, NY). All immunoblotting analyses were performed more than three times.
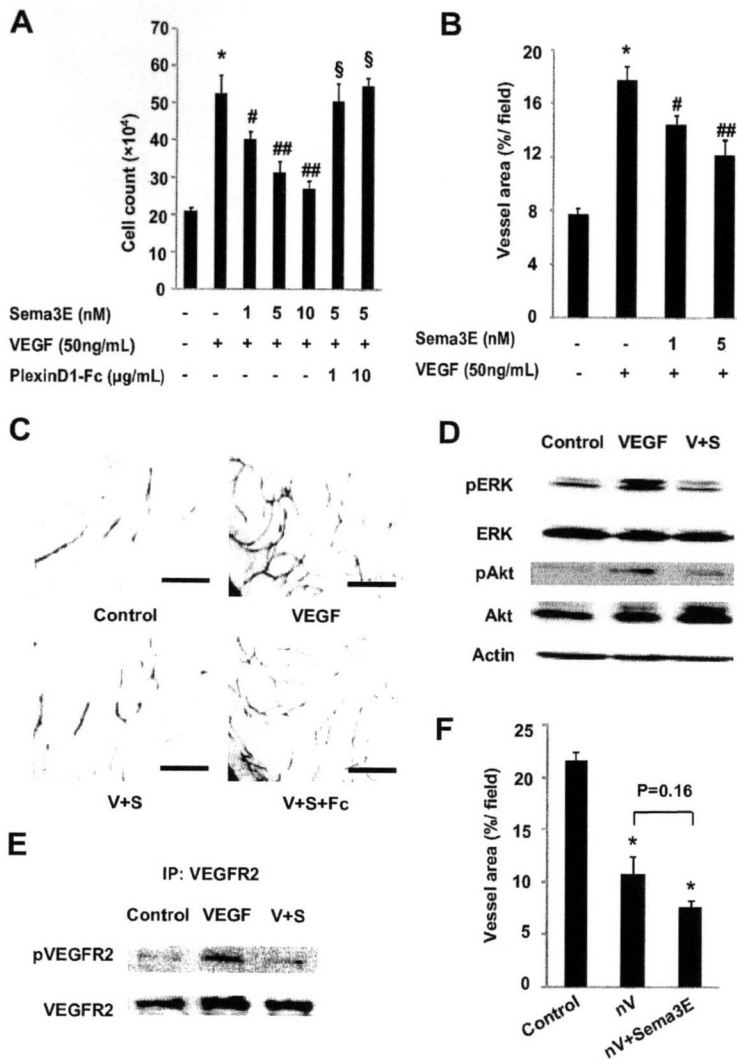
RNA Analysis

Total RNA (30 μg) was extracted by the guanidinium thiocyanate-phenol chloroform method using RNA zol B (Tel Test, Friendswood, Tex) according to the instructions of the manufacturer. cDNA was prepared using the SuperScript First-Strand Synthesis System for RT-PCR (Invitrogen). Quantitative real-time PCR was performed by using the LightCycler (Roche, Indianapolis, Ind) with the TaqMan Universal ProbeLibrary and the LightCycler Master (Roche) according to the instructions of the manufacturer.

Experimental Animals

The animal experiments were approved by our institutional review board. C57/BL6 mice were purchased from the SLC Japan. All mice used in this study were 8 to 12 weeks old. p53-deficient mice (in C57/BL6 background) were purchased from The Jackson Laboratory (Bar Harbor, Me). For the type 1 diabetic model, mice were treated with an intraperitoneal injection of streptozotocin in 0.1 mol/L sodium citrate (pH 4.5) at a dose of 50 mg/kg body weight for 5 days. Generation and genotyping of Sema3E-deficient mice (in C57/BL6 background) have been described previously.[10]

Hindlimb Ischemia Model

After mice were anesthetized, the proximal part of the femoral artery and the distal portion of the popliteal artery were ligated and stripped out after all side branches were dissected free.[16] For in vivo gene transfer, we exposed thigh muscle by excising the skin and injected the expression vector encoding soluble plexinD1-Fc, VEGF, or Sema3E into the muscle twice after surgery. We analyzed blood flow recovery until day 28 after surgery. Hindlimb perfusion was measured with a laser Doppler perfusion analyzer (Moor Instruments, Devon, UK). Ischemic limb samples were harvested for histology on day 10 after surgery. Vastus and rectus femoris muscle tissues were removed from the ischemic limbs after systemic perfusion with PBS and immediately embedded in OCT compound (Sakura Finetechnical). Then, each specimen was snap frozen in liquid nitrogen and cut into 6 μm sections. The sections were stained with antibodies for CD31 (Pharmingen), plexinD1, or Sema3E (Santa Cruz Biotechnology). Two transverse sections of the entire muscle were photographed digitally at a magnification of ×100 (12 to 16 photographs per mouse), and these photographs were reviewed in a blinded manner. Capillary endothelial cells were identified by immunoreactivity for CD31 and quantified as vessel area (%), which was defined as the area of CD31-positive cells/total area.

A

Cell count (×10⁴)

Sema3E (nM)   -   -   1   5   10   5   5
VEGF (50ng/mL) -   +   +   +   +   +   +
PlexinD1-Fc (μg/mL) -   -   -   -   -   1   10

B

Vessel area (% field)

Sema3E (nM)   -   -   1   5
VEGF (50ng/mL) -   +   +   +

C

Control   VEGF

V+S   V+S+Fc

D

Control VEGF V+S

pERK

ERK

pAkt

Akt

Actin

E

IP: VEGFR2

Control VEGF V+S

pVEGFR2

VEGFR2

F

Vessel area (% field)

Control   nV   nV+Sema3E

P=0.16

Figure 1. Sema3E suppresses VEGF-induced angiogenesis. A, Cultured endothelial cells were treated with VEGF alone (50 ng/mL) or VEGF+Sema3E (1, 5, or 10 nmol/L) or VEGF+Sema3E+plexinD1-Fc (1 or 10 μg/mL). Sema3E significantly inhibited VEGF-induced endothelial cell proliferation, which was effectively reversed by plexinD1-Fc treatment. *$P<0.01$ vs Sema3E (−)/VEGF (−)/plexinD1-Fc (−) (n=4); #$P<0.05$, ##$P<0.01$ vs Sema3E (−)/VEGF (+)/plexinD1-Fc (−) (n=4); §$P<0.01$ vs Sema3E (5 nmol/L)/VEGF (+)/plexinD1-Fc (−) (n=4). Data represent means±SEM. B, Endothelial cells cocultured with fibroblasts were treated with VEGF and/or Sema3E for 11 days, and vessel area was assayed by immunohistochemistry for CD31. Sema3E significantly inhibited VEGF-induced tube formation. *$P<0.01$ vs Sema3E (−)/VEGF (−) (n=4); #$P<0.05$, ##$P<0.01$ vs Sema3E (−)/VEGF (+) (n=4). Data represent means±SEM. C, Photographs show tube formation of endothelial cells in the presence of VEGF (50 ng/mL) (VEGF), VEGF+Sema3E (5 nmol/L) (V+S), or VEGF+Sema3E+PlexinD1-Fc (10 μg/mL) (V+S+Fc). Scale bar=300 μm. Vehicle treatment served as control (control). D, Endothelial cells were treated with VEGF (50 ng/mL) (VEGF) or VEGF plus Sema3E (5 nmol/L) (V+S) and analyzed for the VEGF signal pathways by Western blot analysis (n=4). Sema3E suppressed VEGF-induced phosphorylation of ERK (pERK) and Akt (pAkt). Vehicle treatment served as control (control). E, Protein samples prepared in D were analyzed for phospho-VEGFR2 levels (n=7). Sema3E suppressed VEGF-induced phosphorylation of VEGFR2. F, VEGF-induced tube formation was examined in the presence of anti-VEGF antibody (500 μg/mL) (nV), Sema3E (5 nmol/L) (Sema3E), or anti-VEGF antibody plus Sema3E (nV+Sema3E). Vehicle treatment served as control (control). In the presence of anti-VEGF antibody, Sema3E did not significantly inhibit tube formation. *$P<0.01$ vs control (n=4).

Statistical Analysis

Data were shown as means±SEM. Multiple group comparison was performed by 1-way ANOVA followed by the Bonferroni procedure for comparison of means. Comparisons between 2 groups were analyzed by the unpaired Student t test. Values of $P<0.05$ were considered statistically significant.

Results

Sema3E Suppresses VEGF-Induced Angiogenesis in Cultured Endothelial Cells

To investigate the role of Sema3E/plexinD1, we first performed an in vitro study using HUVECs. We seeded HUVECs at 1×10^5 cells per 100-mm-diameter dish and counted the number of cells at 2 days after seeding. Treatment of HUVECs with VEGF markedly increased the cell count (Figure 1A), although this increase was strongly inhibited by addition of Sema3E in a dose-dependent manner (Figure 1A). Treatment with a plexinD1-Fc fusion protein, which binds to Sema3E and inhibits its activity, blocked the effect of Sema3E (Figure 1A). We also performed an angiogenesis assay, in which HUVECs were cocultured with fibroblasts in the presence or absence of Sema3E. When endothelial tube formation was assessed

after 11 days, it was found that treatment with VEGF markedly increased tube formation, although this increase was significantly inhibited by addition of Sema3E (Figure 1B). Treatment with the plexinD1-Fc fusion protein also antagonized the effect of Sema3E on VEGF-induced tube formation (Figure 1C), suggesting that Sema3E is an antiangiogenic factor. We next investigated how Sema3E inhibited angiogenesis. After depriving HUVECs of VEGF for 7 hours, we examined the effect of VEGF treatment. Addition of VEGF induced the phosphorylation of ERK and Akt, both of which are crucial kinases in the intracellular signaling pathway for this growth factor. Pretreatment with Sema3E suppressed VEGF-induced phosphorylation of these two kinases (Figure 1D; Online Figure I, A). Sema3E treatment also suppressed VEGF-induced phosphorylation of VEGF receptor (VEGFR)-2 (Figure 1E; Online Figure I, B). To determine whether the antiangiogenic effect of Sema3E was VEGF-dependent, we next examined the response to addition of an anti-VEGF neutralizing antibody. In the presence of the anti-VEGF antibody, Sema3E did not significantly inhibit cell growth and tube formation (Figure 1F; Online Figure I, C),
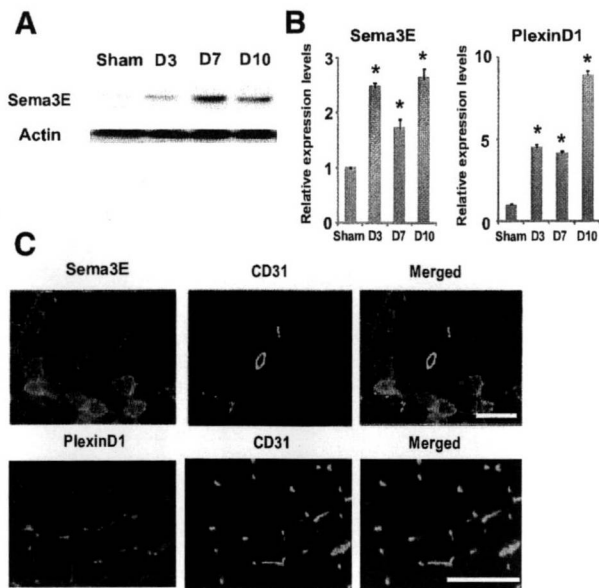
Figure 2. Expression of Sema3E is markedly upregulated in ischemic tissues. A, Western blot analysis for Sema3E expression in ischemic limbs on day 3 (D3), day 7 (D7), and day 10 (D10) after surgery (n=5). Sham indicates sham-operated. B, The mRNA levels of Sema3E and plexinD1 in ischemic limbs on day 3 (D3), day 7 (D7), and day 10 (D10) after surgery were assessed by real-time PCR analysis. *P<0.01 vs sham (n=5). Data represent means±SEM. C, The frozen sections of murine ischemic tissue on day 10 after surgery were subjected to immunofluorescence staining for Sema3E (top) or plexinD1 (bottom) (green). The sections were double-stained with CD31 (red). Scale bar=100 μm.

suggesting that Sema3E negatively regulates angiogenesis by inhibiting the VEGF pathway.

Sema3E Suppresses Angiogenesis In Vivo

To investigate the role of Sema3E/plexinD1 in postnatal angiogenesis, we used a murine model of hindlimb ischemia that was created by unilateral femoral artery ligation. Ischemic tissues were harvested and subjected to Western blot analysis and immunohistochemistry. Expression of Sema3E and plexinD1 was markedly increased in ischemic limbs at 3 days after surgery, and this increase persisted until day 10 (Figure 2A and 2B; Online Figure II). Immunohistochemistry showed that Sema3E was expressed by arterioles, myocytes, and capillary endothelial cells in the ischemic limbs, whereas plexinD1 was mainly expressed by capillary endothelial cells (Figure 2C). To examine whether inhibition of Sema3E promoted angiogenesis, we injected an expression vector encoding the plexinD1-Fc gene into ischemic limbs and analyzed blood flow recovery and the vessel area of the limbs. Laser Doppler perfusion imaging revealed that the plexinD1-Fc group showed significantly better recovery of blood flow than the control group (Figure 3A). Likewise, the vessel area of ischemic limbs at 10 days after surgery was significantly larger in the plexinD1-Fc group than in the control group (Figure 3B; Online Figure III, A).

To further investigate the effect of Sema3E on angiogenesis, we introduced an expression vector encoding the VEGF gene, a vector for the Sema3E gene, or the vectors for both

genes. Injection of the VEGF vector into ischemic limbs significantly accelerated blood flow recovery compared with the control group, whereas this effect was suppressed by coinjection of the Sema3E vector (Figure 3C). In addition, the vessel area was smaller in the Sema3E plus VEGF group than in the VEGF alone group (Figure 3C). Moreover, injection of a vector encoding the plexinD1-Fc gene into ischemic limbs treated with the Sema3E and VEGF vectors significantly improved blood flow recovery and increased the vessel area compared with the findings in the Sema3E plus VEGF group (Figure 3C), suggesting that Sema3E also inhibits neovascularization in ischemic tissue. Next, we created hindlimb ischemia in Sema3E-deficient mice to examine the effect of loss-of-function of this molecule. Consistent with the results of our gene transfer experiments, Sema3E-deficient mice[10] showed better blood flow recovery and a larger vessel area in their ischemic limbs than wild-type mice (Figure 3D; Online Figure III, B). These results indicate that Sema3E/plexinD1 negatively regulate postnatal angiogenesis.

p53 Upregulates Sema3E Expression Both In Vitro and In Vivo

There is evidence that expression of the tumor suppressor protein p53 is increased by hypoxia, thereby inhibiting tumor angiogenesis.[17,18] We identified a putative p53-binding element within the promoter region of the Sema3E gene (data not shown), suggesting that induction of p53 by hypoxia might upregulate Sema3E expression in ischemic limbs. To investigate this hypothesis, we infected HUVECs with an adenoviral vector encoding p53, and then examined Sema3E expression by Western blot analysis. In agreement with our hypothesis, overexpression of p53 led to upregulation of Sema3E expression in HUVECs (Figure 4A). Expression of Sema3E was also induced by treatment with cobalt chloride, which mimics the effects of hypoxia (Figure 4B). To further investigate the relationship between p53 and Sema3E, we next infected HUVECs with a retroviral vector encoding the HPV16 E6 gene, which blocks p53 expression and examined the effect on expression of Sema3E by endothelial cells. Exposure to cobalt chloride for 12 hours markedly upregulated both Sema3E and p53 expression in mock-infected HUVECs, whereas there was no induction of Sema3E expression in E6-infected cells (Figure 4B), suggesting that hypoxia promoted the induction of Sema3E via a p53-dependent pathway.

Consistent with our in vitro data, expression of both p53 and Sema3E was markedly increased in the ischemic limbs of wild-type mice at 3 days after femoral artery ligation (Figures 2A and 4C; Online Figure IV, A). To determine whether Sema3E was regulated by p53 in vivo, we created hindlimb ischemia in p53-deficient mice and wild-type mice and then examined the expression of Sema3E in ischemic limbs. Consistent with our in vitro results, upregulation of Sema3E expression was abolished in the ischemic limbs of p53-deficient mice (Figure 4D; Online Figure IV, B), suggesting that an increase of p53 promotes Sema3E expression in ischemic tissue and thus inhibits blood flow recovery.
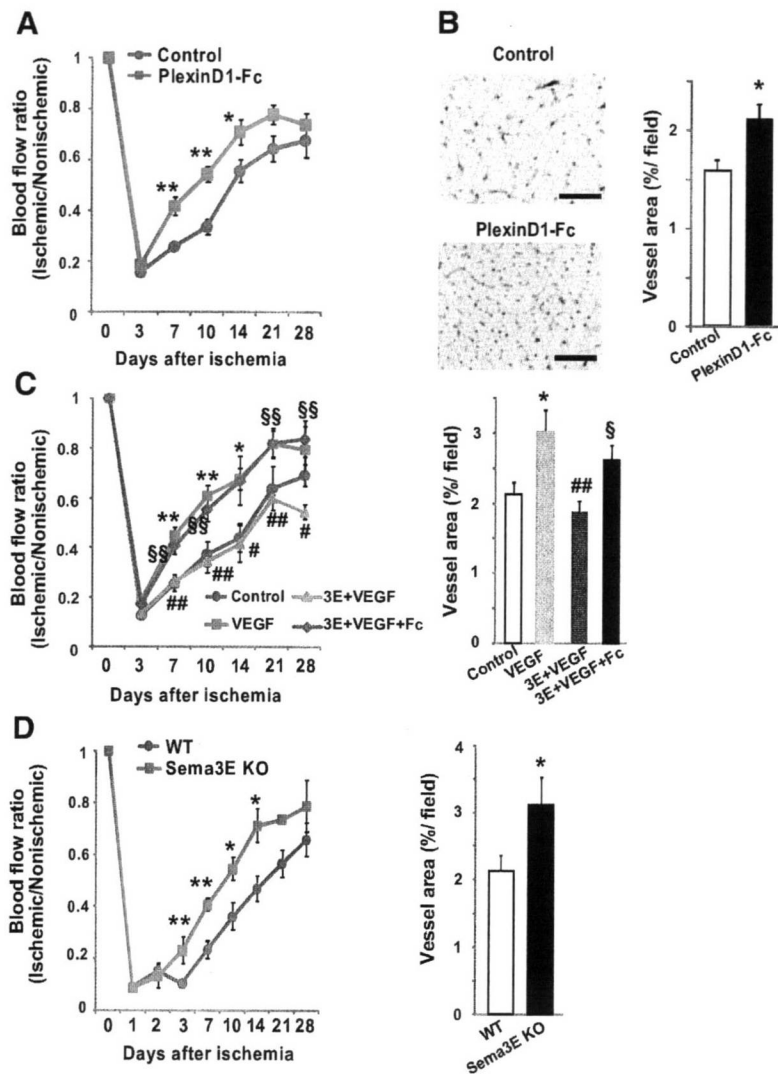
Figure 3. Sema3E negatively regulates angiogenesis in ischemic tissue. A and B, Ischemic limbs of mice were treated with an empty vector (control) or the plexinD1-Fc expression vector (plexinD1-Fc) by intramuscular injection, and blood flow recovery (A) and vessel area (B) were analyzed by laser Doppler perfusion imaging and immunohistochemistry for CD31, respectively. Mice treated with plexinD1-Fc showed better blood flow recovery and a larger vessel area. *$P<0.05$, **$P<0.01$ vs control ($n=8$ for A and B). Data represent means±SEM. Photographs show immunohistochemistry for CD31 in ischemic limbs on 10 days after surgery. Scale bar=100 μm. C, Ischemic limbs of mice were treated with mock (control), the VEGF vector only (VEGF), the Sema3E and VEGF vectors (3E+VEGF), or the Sema3E, VEGF, and plexinD1-Fc vectors (3E+VEGF+Fc), and blood flow recovery (left) and vessel area (right) were analyzed by laser Doppler perfusion imaging and CD31 immunohistochemistry, respectively. Injection of the Sema3E vector into ischemic limbs suppressed VEGF-induced neovascularization, which was effectively reversed by the plexinD1-Fc vector treatment. *$P<0.05$, **$P<0.01$ vs control; #$P<0.05$, ##$P<0.01$ vs VEGF; §$P<0.05$, §§$P<0.01$ vs 3E+VEGF ($n=8$ to 10). Data represent means±SEM. D, Ischemic limbs of wild-type mice (WT) and Sema3E-deficient mice (Sema3E KO) were analyzed for blood flow recovery (left) and vessel area (right). Sema3E-deficient mice showed better blood flow recovery and a larger vessel area of ischemic limbs. *$P<0.05$ vs WT mice ($n=3$ to 8). Data represent means±SEM.

Inhibition of Sema3E Improves Angiogenesis in Diabetic Mice

It has been reported that the angiogenic response to ischemia is attenuated in patients with diabetes.[19] We created a murine model of type 1 diabetes by intraperitoneal injection of streptozotocin (50 mg/kg per day for 5 days) and examined neovascularization after the animals were subjected to hind-limb ischemia. Blood glucose level was significantly higher and blood insulin level was significantly lower in streptozotocin-induced diabetic mice than in control mice (Online Figure V, A). Mice with streptozotocin-induced diabetes also showed poor blood flow recovery and a smaller vessel area in their ischemic limbs compared with control mice (Figure 5A and 5B). To investigate whether the impairment of neovascularization in diabetic mice was related to p53 and Sema3E, we examined the expression of these proteins in the mice. Western blot analysis revealed that p53 expression was increased in diabetic mice and that this increase was further enhanced by ischemia (Figure 5C; Online Figure V, B; and data not shown). Likewise, expression of Sema3E was significantly increased in diabetic mice

compared with control mice (Figure 5C; Online Figure V, B). Consequently, blood flow recovery and the increase of the vessel area after VEGF treatment were significantly impaired in diabetic mice compared with VEGF-treated control mice (Figure 5A and 5B). To further assess the effect of inhibition of Sema3E in diabetic mice, we injected an expression vector encoding the plexinD1-Fc gene into the ischemic limbs of diabetic mice. Laser Doppler perfusion imaging of ischemic limbs and immunohistochemistry for CD31 revealed that the poor response of neovascularization to VEGF treatment was effectively overcome by introduction of the plexinD1-Fc gene (Figure 5D), suggesting that overexpression of Sema3E was responsible for impairment of neovascularization in the diabetic mice. These results indicate that inhibition of Sema3E is effective for promoting angiogenesis, especially when VEGF treatment is ineffective, such as in the diabetic state.

Discussion

The present study demonstrated that the Sema3E/plexinD1 axis inhibits postnatal angiogenesis in a murine model of
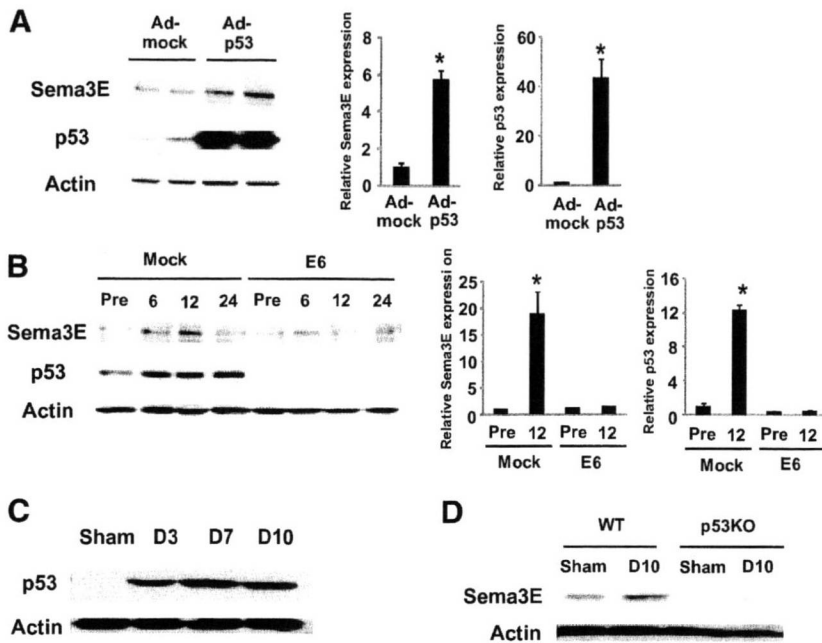
Figure 4. p53 regulates expression of Sema3E. A, Endothelial cells were infected with an adenoviral vector encoding p53 (Ad-p53) or mock (Ad-mock) and subjected to Western blot analysis for expression of Sema3E and p53 (left). Relative expression levels of Sema3E and p53 were plotted in the graph (right). *$P<0.01$ vs Ad-mock (n=4). Overexpression of p53 upregulated Sema3E expression. B, Endothelial cells were infected with a retroviral vector encoding HPV16 E6 (E6) or mock (Mock) and treated with CoCl$_2$ (100 μmol/L) for 6, 12, 24 hours (6, 12, 24). Expression of Sema3E and p53 was examined by Western blot analysis (left). Relative expression levels of Sema3E and p53 were plotted in the graph (right). *$P<0.05$ vs control (Pre) (n=3). Treatment with CoCl$_2$ markedly upregulated Sema3E expression compared to control (Pre), and this upregulation was inhibited by disruption of p53. C, Western blot analysis for p53 expression on day 3 (D3), day 7 (D7), and day 10 (D10) after surgery (n=4). Sham indicates sham-operated. Expression of p53 was markedly upregulated 3 days after surgery, and this upregulation persisted for 10 days. D, Western blot analysis for Sema3E expression in ischemic limbs of wild-type (WT) or p53-deficient (p53KO) mice on day 10 after surgery (n=4). Sema3E expression was increased in ischemic limbs of wild-type mice but not p53-deficient mice.

hindlimb ischemia. Our results also suggested that Sema3E inhibits angiogenesis by blocking activation of the VEGFR-2 and its downstream signaling pathway. Although Sema3E does not bind to neuropilin-1,[10] attraction of axons by Sema3E requires the presence of neuropilin-1 in addition to plexinD1, so the mode of assembly of the ligand and receptor complex is thought to determine the function of Sema3E.[20] Neuropilin-1 also binds to the VEGFR-2 and plays a crucial role in the regulation of VEGF signaling.[21] Accordingly, Sema3E may inhibit VEGF-induced angiogenesis by limiting the availability of neuropillin-1. Because treatment with an anti-VEGF neutralizing antibody did not completely over-
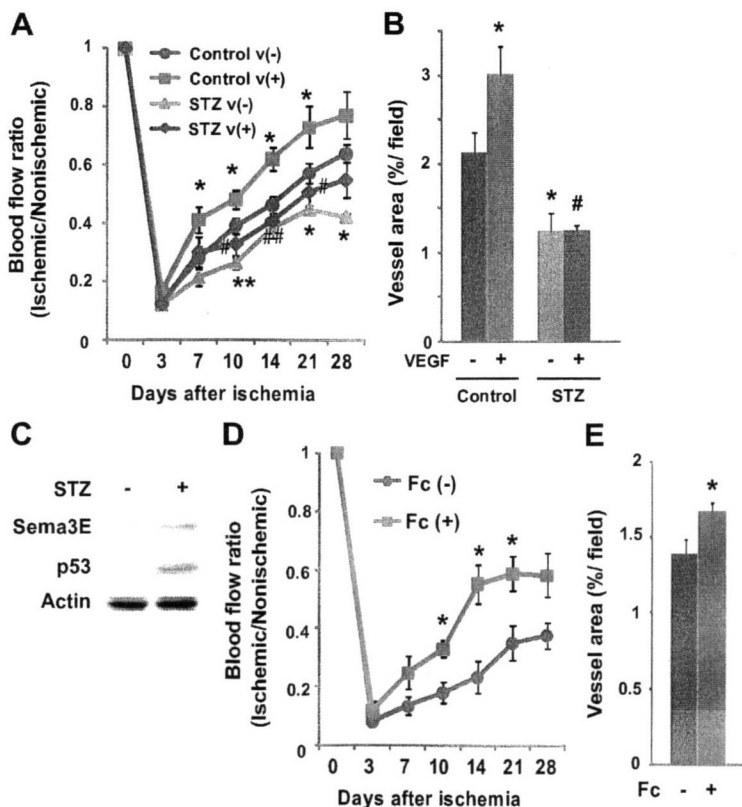
Figure 5. Sema3E inhibition improves impaired angiogenesis in diabetic mice. A and B, Blood flow recovery (A) and vessel area (B) in ischemic limbs of control (control) or streptozotocin-induced diabetic (STZ) mice after treatment with mock [v(−)] or the VEGF expression vector [v(+)]. Diabetic mice showed impaired blood recovery and a smaller vessel area in ischemic limbs compared with control mice. They showed less response to VEGF treatment. *$P<0.05$, **$P<0.01$ vs control/v(−); #$P<0.05$, ##$P<0.01$ vs control/v(+) (n=5 to 12). Data represent means±SEM. C, Expression of Sema3E and p53 was examined in limb tissues of control (STZ−) and streptozotocin-induced diabetic mice (STZ+) by Western blot analysis (n=4). Expression of Sema3E and p53 was upregulated in diabetic mice. D and E, Blood flow recovery (D) and vessel area (E) were analyzed in ischemic limbs of diabetic mice treated with VEGF [Fc(−)] or VEGF+plexinD1-Fc [Fc(+)]. Treatment of plxinD1-Fc in addition to VEGF significantly improved neovascularization in diabetic mice. *$P<0.01$ vs Fc(−) (n=7 to 9). Data represent means±SEM.

come the inhibitory effect of Sema3E on angiogenesis, this effect may also be attributable to the signaling pathway downstream of Sema3E-plexinD1, which is currently unknown.

Sema3E suppressed VEGF-induced phosphorylation of ERK and Akt (Figure 1D). It is well accepted that both ERK and Akt are crucial for the intracellular signaling pathways stimulated by hepatocyte growth factor (HGF) or basic fibroblast growth factor basic (bFGF) to induce angiogenesis. Interestingly, Sema3E also inhibited bFGF or HGF-induced tube formation in a dose-dependent manner (Online Figure VI, A). Moreover, Sema3E significantly inhibited bFGF-induced tube formation even in the presence of the anti-VEGF antibody, whereas it did not inhibit HGF-induced tube formation (Online Figure VI, B). These results suggest that besides the suppression of VEGF-induced angiogenesis, the antiangiogenic effect of Sema3E was partially mediated by VEGF-independent mechanisms.

It is known that intersomitic vessels are disorganized in Sema3E-deficient mice,[10] and this phenotype is markedly similar to that observed in mice lacking plexinD1.[13,14] However, whereas plexinD1-deficient mice develop severe cardiovascular defects involving the outflow tract of the heart and derivatives of the aortic arch arteries that result in perinatal death,[13] Sema3E-deficient mice do not show any large vessel abnormalities and do not undergo embryonic death. PlexinD1 has also been reported to bind to other semaphorins besides Sema3E, such as Sema3A,[13] Sema3C,[22] and Sema4A.[23] It has been shown that Sema3E only binds to plexinD1, whereas Sema3A and Sema3C bind to plexinA1 as well as to plexinD1.[5,10] Sema3A-deficient mice show neural path-finding defects and abnormalities of vascular development that result in neonatal death.[24–26] Ablation of the Sema3C gene in mice results in severe outflow tract abnormalities and mispatterning of intersomitic vessels.[27] Because plexinA1 deficiency also leads to cardiovascular defects,[28] Sema3A/C may play a pivotal role in embryonic vascular development regulated by the plexinA1/D1 pathway. More recently, Sema3A and Sema4A have been shown to inhibit postnatal angiogenesis,[29] suggesting that plexinD1-Fc treatment increases blood flow recovery in ischemic limbs by inhibiting Sema3E but also Sema3A/4A. Sema4D also has an inhibitory effect on postnatal angiogenesis[30]; however, it remains to be determined whether Sema4D binds to plexinD1.

Our results further suggest that p53 has a crucial role in the induction of Sema3E expression in ischemic tissue, although the precise mechanism of how p53 regulates Sema3E expression remains unknown. Because the antiangiogenic activity of p53 is important for tumor suppression, Sema3E/plexinD1 could be a potential target for the treatment of malignancies with p53 mutations. It has been reported that hyperglycemia activates p53 by increasing the production of reactive oxygen species.[31] Thus, p53-induced upregulation of antiangiogenic factors (including Sema3E) is likely to account for the impairment of angiogenesis in patients with diabetes. Therefore, Sema3E/plexinD1 could also be a target for the treatment of ischemic cardiovascular disease in diabetic patients

because conventional therapeutic angiogenesis is not very efficient in this patient population.[32,33]

Disclosures
None.

References
1. Carmeliet P, Tessier-Lavigne M. Common mechanisms of nerve and blood vessel wiring. *Nature*. 2005;436:193–200.
2. Dickson BJ. Molecular mechanisms of axon guidance. *Science*. 2002; 298:1959–1964.
3. Weinstein BM. Vessels and nerves: marching to the same tune. *Cell*. 2005;120:299–302.
4. Eichmann A, Le Noble F, Autiero M, Carmeliet P. Guidance of vascular and neural network formation. *Curr Opin Neurobiol*. 2005;15:108–115.
5. Neufeld G, Kessler O. The semaphorins: versatile regulators of tumour progression and tumour angiogenesis. *Nat Rev Cancer*. 2008;8:632–645.
6. Luo Y, Raible D, Raper JA. Collapsin: a protein in brain that induces the collapse and paralysis of neuronal growth cones. *Cell*. 1993;75:217–227.
7. Tamagnone L, Artigiani S, Chen H, He Z, Ming GI, Song H, Chedotal A, Winberg ML, Goodman CS, Poo M, Tessier-Lavigne M, Comoglio PM. Plexins are a large family of receptors for transmembrane, secreted, and GPI-anchored semaphorins in vertebrates. *Cell*. 1999;99:71–80.
8. Ohta K, Mizutani A, Kawakami A, Murakami Y, Kasuya Y, Takagi S, Tanaka H, Fujisawa H. Plexin: a novel neuronal cell surface molecule that mediates cell adhesion via a homophilic binding mechanism in the presence of calcium ions. *Neuron*. 1995;14:1189–1199.
9. Song H, Ming G, He Z, Lehmann M, McKerracher L, Tessier-Lavigne M, Poo M. Conversion of neuronal growth cone responses from repulsion to attraction by cyclic nucleotides. *Science*. 1998;281:1515–1518.
10. Kruger RP, Aurandt J, Guan KL. Semaphorins command cells to move. *Nat Rev Mol Cell Biol*. 2005;6:789–800.
11. Roth L, Koncina E, Satkauskas S, Cremel G, Aunis D, Bagnard D. The many faces of semaphorins: from development to pathology. *Cell Mol Life Sci*. 2009;66:649–666.
12. Christensen CR, Klingelhofer J, Tarabykina S, Hulgaard EF, Kramerov D, Lukanidin E. Transcription of a novel mouse semaphorin gene, M-semaH, correlates with the metastatic ability of mouse tumor cell lines. *Cancer Res*. 1998;58:1238–1244.
13. Gitler AD, Lu MM, Epstein JA. PlexinD1 and semaphorin signaling are required in endothelial cells for cardiovascular development. *Dev Cell*. 2004;7:107–116.
14. Torres-Vazquez J, Gitler AD, Fraser SD, Berk JD, Van NP, Fishman MC, Childs S, Epstein JA, Weinstein BM. Semaphorin-plexin signaling guides patterning of the developing vasculature. *Dev Cell*. 2004;7:117–123.
15. Minamino T, Mitsialis SA, Kourembanas S. Hypoxia extends the life span of vascular smooth muscle cells through telomerase activation. *Mol Cell Biol*. 2001;21:3336–3342.
16. Couffinhal T, Silver M, Zheng LP, Kearney M, Witzenbichler B, Isner JM. Mouse model of angiogenesis. *Am J Pathol*. 1998;152:1667–1679.
17. Harris SL, Levine AJ. The p53 pathway: positive and negative feedback loops. *Oncogene*. 2005;24:2899–2908.
18. Teodoro JG, Parker AE, Zhu X, Green MR. p53-mediated inhibition of angiogenesis through up-regulation of a collagen prolyl hydroxylase. *Science*. 2006;313:968–971.

19. Falanga V. Wound healing and its impairment in the diabetic foot. *Lancet.* 2005;366:1736–1743.

20. Chauvet S, Cohen S, Yoshida Y, Fekrane L, Livet J, Gayet O, Segu L, Buhot MC, Jessell TM, Henderson CE, Mann F. Gating of Sema3E/ PlexinD1 signaling by neuropilin-1 switches axonal repulsion to attraction during brain development. *Neuron.* 2007;56:807–822.

21. Soker S, Takashima S, Miao HQ, Neufeld G, Klagsbrun M. Neuropilin-1 is expressed by endothelial and tumor cells as an isoform-specific receptor for vascular endothelial growth factor. *Cell.* 1998;92:735–745.

22. Banu N, Teichman J, Dunlap-Brown M, Villegas G, Tufro A. Semaphorin 3C regulates endothelial cell function by increasing integrin activity. *FASEB J.* 2006;20:2150–2152.

23. Toyofuku T, Yabuki M, Kamei J, Kamei M, Makino N, Kumanogoh A, Hori M. Semaphorin-4A, an activator for T-cell-mediated immunity, suppresses angiogenesis via Plexin-D1. *EMBO J.* 2007;26:1373–1384.

24. Behar O, Golden JA, Mashimo H, Schoen FJ, Fishman MC. Semaphorin III is needed for normal patterning and growth of nerves, bones and heart. *Nature.* 1996;383:525–528.

25. Taniguchi M, Yuasa S, Fujisawa H, Naruse I, Saga S, Mishina M, Yagi T. Disruption of semaphorin III/D gene causes severe abnormality in peripheral nerve projection. *Neuron.* 1997;19:519–530.

26. Serini G, Valdembri D, Zanivan S, Morterra G, Burkhardt C, Caccavari F, Zammataro L, Primo L, Tamagnone L, Logan M, Tessier-Lavigne M, Taniguchi M, Puschel AW, Bussolino F. Class 3 semaphorins control vascular morphogenesis by inhibiting integrin function. *Nature.* 2003; 424:391–397.

27. Feiner L, Webber AL, Brown CB, Lu MM, Jia L, Feinstein P, Mombaerts P, Epstein JA, Raper JA. Targeted disruption of semaphorin 3C leads to persistent truncus arteriosus and aortic arch interruption. *Development.* 2001;128:3061–3070.

28. Toyofuku T, Zhang H, Kumanogoh A, Takegahara N, Suto F, Kamei J, Aoki K, Yabuki M, Hori M, Fujisawa H, Kikutani H. Dual roles of Sema6D in cardiac morphogenesis through region-specific association of its receptor, Plexin-A1, with off-track and vascular endothelial growth factor receptor type 2. *Genes Dev.* 2004;18:435–447.

29. Maione F, Molla F, Meda C, Latini R, Zentilin L, Giacca M, Seano G, Serini G, Bussolino F, Giraudo E. Semaphorin 3A is an endogenous angiogenesis inhibitor that blocks tumor growth and normalizes tumor vasculature in transgenic mouse models. *J Clin Invest.* 2009;119: 3356–3372.

30. Sun Q, Zhou H, Binmadi NO, Basile JR. Hypoxia inducible factor-1-mediated regulation of Semaphorin 4D affects tumor growth and vascularity. *J Biol Chem.* 2009;284:32066–32074.

31. Brodsky SV, Gealekman O, Chen J, Zhang F, Togashi N, Crabtree M, Gross SS, Nasjletti A, Goligorsky MS. Prevention and reversal of premature endothelial cell senescence and vasculopathy in obesity-induced diabetes by ebselen. *Circ Res.* 2004;94:377–384.

32. Losordo DW, Dimmeler S. Therapeutic angiogenesis and vasculogenesis for ischemic disease. Part I: angiogenic cytokines. *Circulation.* 2004;109: 2487–2491.

33. Losordo DW, Dimmeler S. Therapeutic angiogenesis and vasculogenesis for ischemic disease. Part II: cell-based therapies. *Circulation.* 2004;109:2692–2697.